

PAPER • OPEN ACCESS

FLASH radiotherapy and the associated dosimetric challenges

To cite this article: S Ceberg *et al* 2023 *J. Phys.: Conf. Ser.* **2630** 012010

View the [article online](#) for updates and enhancements.

You may also like

- [Mitigating the impact of FLASH-model uncertainties through personalized FLASH optimization functions for delivery pattern optimization for lung IMPT](#)
Manon C van Zon, Sebastiaan Breedveld, Mischa S Hoogeman et al.
- [Mathematical analysis of FLASH effect models based on theoretical hypotheses](#)
Ankang Hu, Wanyi Zhou, Rui Qiu et al.
- [FLASH radiotherapy sparing effect on the circulating lymphocytes in pencil beam scanning proton therapy: impact of hypofractionation and dose rate](#)
Antje Galts and Abdelkhalek Hammi

FLASH radiotherapy and the associated dosimetric challenges

S Ceberg¹, A Mannerberg¹, E Konradsson¹, M Blomstedt¹, M Kügele², M Kadhim^{1,2}, A Edvardsson², S Å J Bäck^{1,2}, K Petersson^{2,3}, C Jamtheim Gustafsson² and C Ceberg¹

¹Department of Medical Radiation Physics, Lund University, Lund, Sweden

²Radiation Physics, Department of Hematology, Oncology and Radiation Physics, Skåne University Hospital, Lund, Sweden

³Oxford Institute for Radiation Oncology, Department of Oncology, University of Oxford, Oxford, UK

E-mail: sofie.ceberg@med.lu.se

Abstract. At Lund University and Skåne University Hospital in Lund, Sweden, we have, as the first clinic, modified a clinical Elekta Precise linear accelerator for convertible delivery of ultra-high dose rate (FLASH) irradiation. Whereas recently published reviews highlighted the need for standardised protocols for ultra-high dose rate beam dosimetry to be able to determine the true potential of FLASH irradiation, several dosimetry studies as well as *in-vitro* and *in-vivo* experiments have been carried out at our unit. Dosimetric procedures for verification of accurate dose delivery of FLASH irradiation to cell cultures, zebrafish embryos and small animals have been established using radiochromic films and thermo-luminescent dosimeters. Also, recently the first experience of electron FLASH radiotherapy (FLASH-RT) in canine patients in our clinical setting was published. Our research facilities also include a laboratory for 3D polymer gel manufacturing. Recently, we started investigating the feasibility of a NIPAM polymer gel dosimeter for ultra-high dose rate dosimetry. Furthermore, in the bunker of the modified Elekta linear accelerator, a Surface Guided Radiotherapy (SGRT) system is accessible. The Catalyst™ system (C-Rad Positioning, Uppsala, Sweden) provides optical surface imaging for patient setup, real-time motion monitoring and breathing adapted treatment. Aiming at treating patients using ultra-high dose rates, a real-time validation of the alignment between the beam and the target is crucial as the dose is delivered in a fraction of a second. Our research group has during the last decade investigated and developed SGRT workflows which improved patient setup and breathing adapted treatment for several cancer patient groups. Recently, we also started investigating the feasibility of a real-time motion monitoring system for surface guided FLASH-RT. Both FLASH related studies; 3D polymer gel dosimetry and surface guided FLASH-RT are to our knowledge the first of their kind. Following an introduction to the field of FLASH and the associated dosimetric challenges, we here aim to present the two ongoing studies including some preliminary results.

1. Introduction

The paradigm of radiotherapy is to irradiate the tumour or treatment volume with high absorbed dose and simultaneously avoid healthy surrounding tissues as much as possible. Due to the last decades of technical development within the radiotherapy workflow, we can aim at the tumour more accurately and thus decrease the absorbed dose to the surrounding healthy tissues. Examples of these technical developments are multi-diagnostic imaging for tumour and organs at risk definition, intensity modulated



beams and arcs, real-time image guidance to continually follow the target during beam-on, and deformable motion models that enable daily adaptive treatment. These technical advances have not only decreased the acute and long-term radiation-induced side effects but also allowed treatments that otherwise would result in intolerable normal tissue complications for the patients. State-of-the-art treatments such as gated stereotactic body radiation therapy (SBRT) liver treatment in an MR-linac workflow [1] and ventricular tachycardia radiotherapy, delivering single 25 Gy fraction during cardiobreathing motion [2], are notable results from the latest generation of technical and methodical developments. However, even with a perfect treatment technique using the current clinical accelerators, the tumour will still be surrounded by healthy tissue. To further improve radiotherapy, we need to increase the therapeutic window by considering other treatment concepts, i.e., to decrease the probability of normal tissue complication and increase/maintain the probability of tumour control.

The novel ultra-high dose rate FLASH irradiation is such a suggestion. The term FLASH was put on the map by Favaudon et al. 2014, presenting experiments carried out using a high-dose-per-pulse 4.5 MeV electron beam with an average dose rate larger than 40 Gy/s, which is at least hundred times higher than conventionally used in radiotherapy [3]. Pre-clinical FLASH studies have shown promising results, indicating a possibility to increase the therapeutic window [3]. The evidence for this so-called FLASH effect has started to accumulate and according to recent reviews, over 25 studies showed data on less normal tissue toxicity than conventional radiotherapy, of which over 10 studies also investigated and showed data on maintained similar tumour effect [4-6]. The in-vivo studies involved irradiation of zebrafishes, small animals, and mini pigs, but also veterinary canine and feline patients. The overall result showed that short beam-on time (<200 ms), and large single doses (≥ 10 Gy) can protect normal tissue by 20-40 % compared to conventional radiotherapy [3,7-15], without compromising the intended treatment effect [3,9,11,13]. The results showed less DNA damage and cell death in the normal tissue as well as less chronic inflammation and vascular damages compared to conventional RT. Furthermore, the studies show preserved function in the skin but also in cognitive functions. And in the meantime, according to another recent published review, a maintained similar tumour control (tumour growth) was demonstrated [16].

These results might enable possibilities for treatments of patients with more radioresistant tumours that are not cured today, or not even considered for radiotherapy, due to the risk of intolerable normal tissue complications.

2. Challenges in ultra-high dose rate beam dosimetry

Today the fundamental underlying physiochemical and radiobiological mechanisms for the FLASH effect are not yet fully understood and are currently under investigation [17]. Several laboratories have established the biological response and showed robustness of their experiments, however differences in the magnitude of the FLASH effect between laboratories have been reported [17]. In the two recently published special issue papers; Schüler et al. 2022 and Romano et al. 2022, the authors proclaim that we need to establish standardised protocols for ultra-high dose rate (UHDR) beam dosimetry to be able to determine the true potential of FLASH irradiation and thus finally move towards clinical translation [17,18]. The suggested required parameters are, among others, beam energy and time structure, total dose, mean dose rate, intra-pulse dose rate, pulse repetition frequency, dose-per-pulse, and pulse width [17]. Also, established methods for absorbed dose measurement and real-time output monitoring of UHDR beams need to be properly addressed [18]. An initiative to develop and improve dosimetry standards for FLASH radiotherapy was recently carried out by the European Joint Research Project UHDPulse [19]. However, currently, no recommendation for UHDR dosimetry is available, as TRS 398 and TG51 are for dosimetry of conventional radiotherapy.

Conventionally used measurement methods and detector systems have shown to be heavily affected by the dose rate and dose-per-pulse characteristic for UHDR irradiation [18]. For instance, ionization chambers, considered the gold standard detector for conventional radiotherapy dosimetry, suffer from significant ion recombination effects at FLASH irradiation dose rates, resulting in a dose rate dependence [20-22]. The Si-based semi-conductor detectors already suffer from dose rate

dependence using conventional dose rates, and also beam angular dependence, long term irradiation damage and non-tissue equivalence [20]. Radiochromic film has on the other hand tissue equivalent dosimetric properties and high spatial resolution, however, the detector shows an LET dependence and cannot provide real-time measurements [18]. Nevertheless, these conventionally used detector systems available in a radiotherapy clinic have been shown to also be feasible for UHDR dosimetry, however, with careful consideration regarding corrections and calibrations. There are however numerous promising novel studies presenting other detector candidates for dosimetry of UHDR beams [20].

2.1 Charge-based dosimeters

The function of most charge-based detectors is based on the principle that the irradiation creates ion pairs or charges, which are collected and then correlated to absorbed dose. Ionisation chamber, Faraday Cup, and the solid-state detectors such as diamonds and diodes are examples on charge-based detectors. The advantages, having UHDR beam dosimetry in mind, are the detectors' high time resolution, in the range of ns-ms, which makes them suitable for real-time dosimetry, however, they are limited to point-dose measurements. Typical unfavourable characteristics for charge-based detectors are their dose rate- and energy dependence and non-tissue equivalence. Several promising modifications to meet the demands of the UHDR beam dosimetry have however recently been investigated for ion chambers and diamond detectors [23-26]. For instance, ion recombination correction model has been suggested by Cavallone et al. 2022 for online dosimetry using a Nano Chamber, and Gómez et al. 2022 demonstrated the ability to extend the dose rate operating range of an ultra-thin parallel plate ionization chamber by reducing the spacing between electrodes [23,24]. Furthermore, novel approaches for the feasibility of a diamond detector for UHDR beam dosimetry have also been carried out recently. Kranzer et al. 2022 showed that the linear range can be extended towards a higher dose-per-pulse range by reducing the active volume and thus the sensitivity [25]. Marinelli et al. 2022 showed the same but by fine-tuning other physical properties of the diamond detector such as the resistance [26].

2.2 Luminescent dosimeters

Any system which utilises optical photon generation upon irradiation and where the measured light correlates to the absorbed dose, belongs to the group of luminescent dosimeters. Examples of luminescent dosimeters are thermo-luminescent detectors (TLD), optically stimulated luminescent detectors (OSLD), and the Cherenkov detector [18,20]. Some crystals absorb and trap energy due to added impurities in the crystal lattice when exposed to irradiation. When heated (TLD) or optically stimulated (OSLD), the crystal releases the trapped energy in the form of visible light, which correlates to the accumulated absorbed dose. These luminate detectors have been used for UHDR beam dosimetry for a long time, due to their excellent dose rate independence and tissue equivalence. Additionally, TLD can be manufactured to be small, or in powder form, which allows for high spatially-resolved measurements. Although the detectors are passive, they have been used in several dosimetric validation studies for FLASH RT [27,28]. The Cherenkov dosimeter is an active luminescent detector. When charged particles travel at a phase velocity that exceeds the phase velocity of light in the irradiated medium, Cherenkov irradiation is emitted, where the intensity of light is proportional to absorbed dose [29]. Investigated Cherenkov based detector systems show characteristics such as high time resolution (prompt, ps), linear to absorbed dose, and dose rate independent [20], which suggest the detector to be an excellent candidate for clinical 2D real-time UHDR beam dosimetry [30]. However, Cherenkov based detector systems are expected to be energy dependent and determining the relation between light yield and absorbed dose can be complicated under experimental conditions. Intensive research is ongoing [20,31].

2.3 Chemical dosimeters

Any system that produces radicals, change colour, or undergo structural changes when irradiated, and where the measured transformation correlates to the absorbed dose, belongs to the group of chemical dosimeters. Typically, the chemical dosimeter forms stable radiation-induced changes which can be

read-out using optical laser, magnetic resonance imaging, or electron paramagnetic resonance spectroscopy [18]. Two frequently used chemical dosimeters in published pre-clinical FLASH studies are radiochromic films and alanine. Also, these two detectors were used for dose validation for the first human treated with FLASH-RT [32]. Alanine is an amino acid which forms a stable free radical upon irradiation. Electron paramagnetic resonance spectroscopy is then used to measure the amount of stable free radicals, which is proportional to the absorbed dose [33]. Alanine dosimeters exhibit linear dose response over a large range (2-150,000 Gy) and shows dose rate independence up to the order of magnitude 10^{10} Gy/s [20]. These characteristics make the alanine dosimeter very useful in UHDR beam dosimetry [33], although the detector is a passive system, and the resolution is limited to the size of the pellets [20]. Radiochromic film is close to the passive ideal detector system with very high resolution in 2D, both energy- and dose rate-independent, as well as tissue equivalence. The disadvantage is that the read-out is recommended to be carried out 16-24 h post irradiation due to continued post-exposure polymerisation [18,20,28,34].

True 3D chemical dosimeters, such as polymer gel detectors, might be suitable detectors for UHDR beam dosimetry due to the high spatial resolution, energy independence, and tissue equivalence. The drawback is a known dose rate dependence [35,36]. The polymer gel dosimeter has been considered as a suitable candidate [20], however, a polymer gel FLASH study has not yet been reported.

Right dose in right place

Suppose we now have established standardised protocols for UHDR beam dosimetry and have access to active detector systems with ideal characteristics such as dose rate- and energy independence, tissue-equivalence, and high spatial- and time resolution. Then, another dosimetric challenge emerges, which is to validate that the absorbed dose is delivered to the correct position.

Motion management in radiotherapy is crucial for an accurate dose delivery [37]. The intra-fractional motion of tumour and organs at risks are the most addressed challenges during conventional motion management radiotherapy. With FLASH-RT the intra-fractional motion is nearly eliminated as the dose is delivered in a fraction of a second. However, there is a new demand on motion management, since during this short delivery time a real-time validation of the alignment between the beam and the target is crucial. Image guidance is standard in radiotherapy to verify the patient setup and adapt the treatment plan in the event of any anatomical changes. For FLASH-RT, the ultrafast delivery demands state-of-the-art image guidance. For superior soft tissue contrast, MR-images would be ideal, however this is not yet available in combination with FLASH-RT. El Naqa et al. 2022 argues that future multiparametric on-board MRI protocols also could include functional information that could be explored in combination with FLASH-RT [31]. As for today, the widely accessible on-board imaging system is cone beam computed tomography (CBCT), which provides 3D volumetric kilovoltage imaging of the patient and has shown to reduce localization errors in radiotherapy by approximately 50% [38]. Recent developments in radiotherapy combine volumetric imaging with surface guided radiotherapy (SGRT) [39].

Real-time motion monitoring

Motion management systems using optical surface imaging, so called SGRT, are used clinically for patient positioning and real time motion monitoring and have been suggested to be a potential candidate for motion management system at FLASH-RT [31,40].

SGRT provides the largest available field-of-view (FOV) in radiotherapy [41] with approximately 1 m^3 scanning volume [42]. The capability to capture surface images of the patient in real-time makes SGRT systems excellent for motion management. The Catalyst™ system is an optical surface scanning system that consists of a high-power LED projector, which projects a near-visible violet light ($\lambda=405 \text{ nm}$) for surface reconstruction purposes and a green ($\lambda=528 \text{ nm}$) and red ($\lambda=624 \text{ nm}$) projection light for live feedback of the patient posture position. The Catalyst™ is a structured light system, which means that the near-visible violet light is projected as sequenced lines onto the object to be scanned. The irregularity of the object scanned disperses the sequenced lines, which are detected by a CCD camera.

Due to fixed geometry between the projector and the CCD, the principle of optical triangulation can be used to reconstruct a 3D surface of the scanned object. During treatment delivery the surface imaging system monitors the patient motion. The motion of the patient surface is recorded and tolerances for the detected motion are set prior to treatment. The optical surface scanning system is interfacing with the delivery control system to interrupt the beam delivery if the patient motion exceeds any pre-defined tolerance. According to the American Association of Physics in Medicine (AAPM) Task Group Report 142, the latency of beam-on/-off should be within 100 ms for a linac with synchronization of the radiation beam [43]. However, in the case of motion monitoring during FLASH-RT the latency must be much quicker, within a few ms, to be able to turn the beam off during a sudden motion.

3. Two ongoing studies at our FLASH linac

3.1 UHDR beam dosimetry using a polymer gel detector

Three-dimensional (3D) gel dosimetry has played an important role when introducing new treatments techniques into the radiotherapy clinic, such as IMRT/VMAT and breathing adapted conformal treatments [44,45,46]. All polymer gel dosimetry systems are characterized by polymerization, induced locally by free radical products of water radiolysis. The polymerization alters due to various physical and chemical properties of the polymer gel system. The 3D absorbed dose map can, for example, be read-out using MRI, optical- or x-ray computed tomography (CT).

The 3D polymer gel dosimeter is a linac-independent stand-alone detector system, tissue-equivalent, has high resolution in 3D, can be mould into various forms, and shows no energy- or beam-angle dependence [45]. However, a LET-dependence and a dose rate dependence have been identified [35,36]. Another disadvantage is that the read-out is recommended to be carried out about 24 h post irradiation due to continued post exposure polymerisation, and that each batch needs to be calibrated. We plan to investigate the possibilities of using electron-range modulating bolus in FLASH-RT and our ambition is to use 3D dosimetry for verification of the dose distribution. The initial aim was to investigate the feasibility of the NIPAM polymer gel detector for UHDR beam dosimetry.

NIPAM gel dosimeters were manufactured in a fume cupboard under normal levels of oxygen using 3 % w/w NIPAM (97 % Sigma-Aldrich), 3 % w/w BIS (99 % Sigma-Aldrich) [36]. Gelatine was used as the matrix substance and tetrakis(hydroxymethyl)-phosphonium chloride as an oxygen scavenger. The remaining constituent was water. The gel mixture was poured into vials of 15 ml (\varnothing 1.5 cm, length 6 cm) and stored in the dark at room temperature for about 24 h before irradiation. The vials from the same batch were irradiated to the same total doses at the convertible clinical Elekta Precise linac with a 10 MeV electron beam (Figure 1), either using conventional dose rate of 0.15 Gy/s or using UHDR (2 Gy/pulse, pulse dose rate = $0.6 \cdot 10^6$ Gy/s, average dose rates ≥ 75 Gy/s, total treatment times ≤ 0.22 s) [47]. All vials were irradiated at a 65 cm source to surface distance (SSD). The experiment was repeated once [48]. Radiochromic film (GafChromic EBT-XD) and a flatbed scanner for read-out (Epson Expression 12000XL) was used for validation of the dose to the gel dosimeters. Small pieces of film were placed into separate water-filled vials. The vials were irradiated with the 10 MeV electron beam, delivering 3, 7, 11 or 17 pulses at ultra-high dose rate or with 291, 679, 1068 or 1650 MU at conventional dose rate.

After irradiation the vials were stored in the dark at room temperature for about 24 h before MRI read-out. The vials were scanned at a General Electric (GE) Architect 3T camera using FSE pulse sequence with a TR 4000 ms and in plane pixel size 0.4×0.4 mm² with a slice thickness of 10 mm [39]. The data processing was carried out using MICE Toolkit 2021.2.1 (NonPi, Sweden). The average pixel intensity as a function of TE_{eff} was plotted for all vials. A mono-exponential curve fit was made to obtain the R2 values.

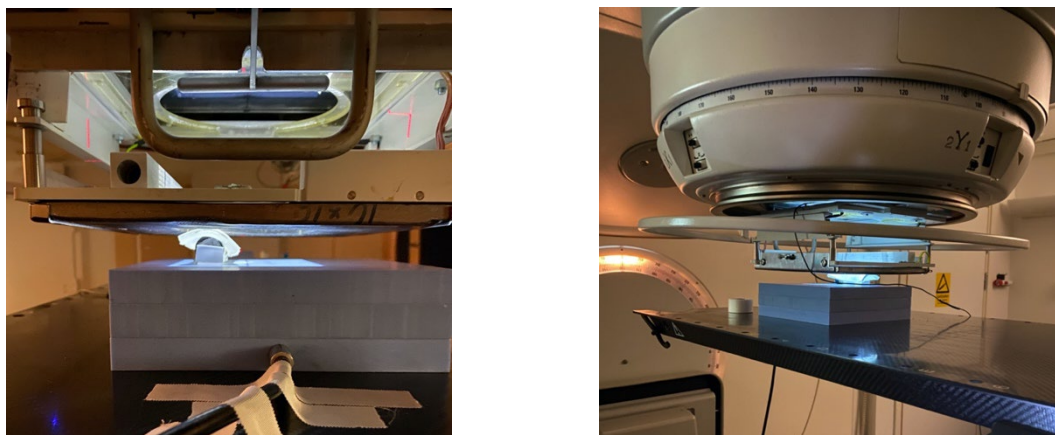


Figure 1. The setup of a polymer gel dosimeter during the electron beam at the convertible clinical Elekta Precise linac. The same setup was used for FLASH as for conventional irradiation.

The measurements carried out using Radiochromic film showed a linear relationship between absorbed dose and number of pulses for the ultra-high dose rate irradiation, and number of MU for conventional dose rate irradiation, respectively (Figure 2). The result enabled us to present the NIPAM gel MR readout signal R2 as a function of absorbed dose (Figure 3).

Gel measurements showed lower response for the ultra-high dose rate irradiation than conventional dose rate irradiation, regardless dose interval investigated, which reveals the detector dose rate dependence. However, the dosimeters did not seem to saturate even at the highest doses investigated (>45 Gy) (Figure 3), which was promising. These data follow a quadratic polynomial trend with $R^2 > 0.99$ for all measurements presented (Figure 3). For absorbed doses up to 25 Gy a linear fit gives $R^2 > 0.98$, which makes it possible to use a NIPAM gel dosimeter to measure relative absorbed dose distributions in that dose range, by using only background subtraction.

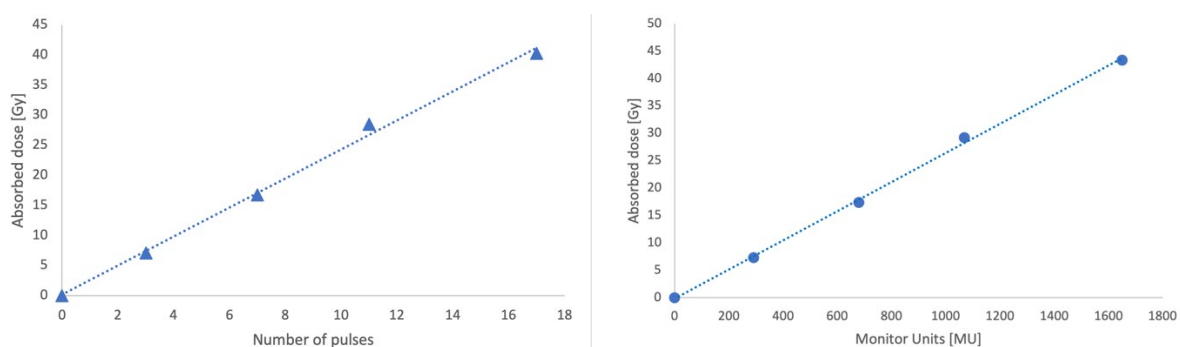


Figure 2. Radiochromic film dosimetry results for 10 MeV electron beam. Measured absorbed dose show a linear relationship to the number of pulses for ultra-high dose rate irradiation, $R^2 > 0.99$ (left panel) and to the number of MU for conventional dose rate irradiation, $R^2 > 0.99$ (right panel).

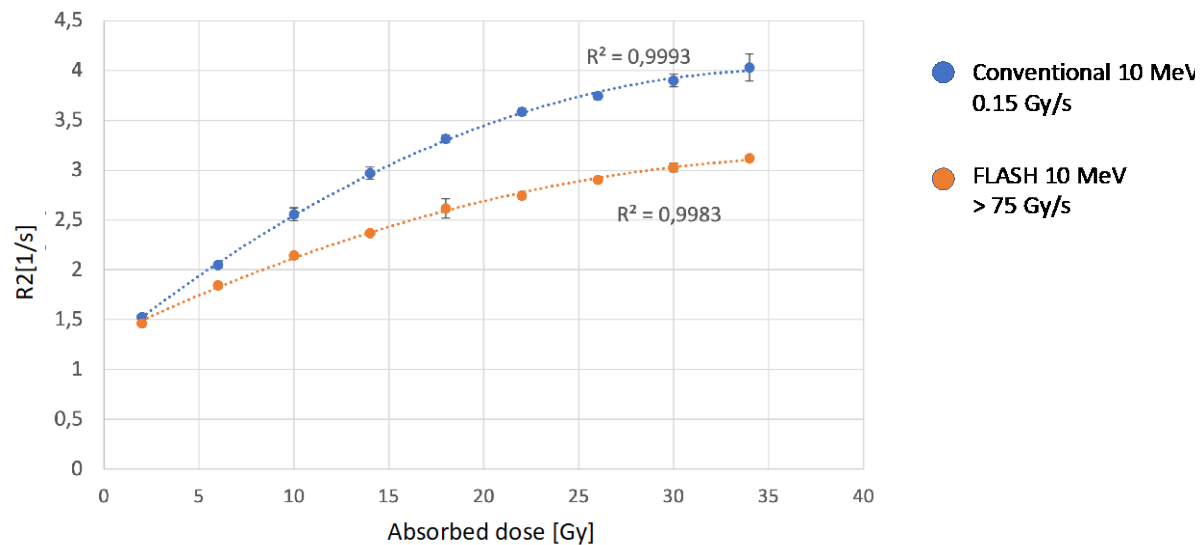


Figure 3. NIPAM polymer gel MR-redout signal R2 as a function of absorbed dose for conventional dose rate (blue) and ultra-high dose rate (orange) 10 MeV electron beam, respectively.

Our preliminary results showed a dose rate dependence, which speaks against the NIPAM gel dosimeter to be an ideal candidate for UHDR beam dosimetry. Nevertheless, relative dosimetry might be possible with a suitable calibration method. The investigation of using NIPAM polymer gel for 3D dose verification of electron-range modulated FLASH-RT is ongoing.

3.2 Surface guided FLASH radiotherapy

The fast FLASH-RT delivery almost eliminates any intra-fractional motion, nevertheless, it is crucial to have proper motion management to ensure a precise and accurate delivery of the potentially very high fraction dose. To enable a successful clinical translation of FLASH-RT, we need the ability to monitor the patient and target position in real-time and verify that the radiation is delivered to the target. Surface guided radiotherapy (SGRT) is a motion management alternative that provides real-time motion monitoring, sub-millimeter accuracy and a large off-isocentric field of view (FoV) [41,42]. Our research group has developed SGRT workflows and improved patient setup and breathing adapted treatment for several cancer patient groups [49-53], and we aim to use SGRT as part of our facility's canine patient research program in electron beam FLASH-RT [15]. As a critical component to the research, the surface imaging system will verify that the dog maintains stable in the correct position when the beam is triggered. However, since the surface imaging system is developed to detect light reflected from a human patient surface at a conventional SSD during conventional treatment times, our aim was to carry out feasibility studies to investigate the performance of the SGRT system for furry patients in a FLASH-RT setting [40].

Phantom studies were carried out using fur-like blankets of various colours placed on a platform which simulated breathing patterns (QUASAR Phantom, Modus Medical Devices). A breathing motion of 15 breaths/min and 10 mm amplitude was simulated and the capability of the surface imaging Catalyst™ system to correctly monitor the motion was investigated in SSD 100 cm, and in our off-isocentric electron FLASH setup at SSD 70 cm. Furthermore, to investigate how accurately the surface imaging system can detect a potential sudden patient related motion during FLASH-RT setup, an in-house moving phantom was utilized. The phantom uses a platform with a programmable vertical motion controlled by a solenoid, which enables the platform to move in a binary pattern. The same fur-like blankets were used and the preset vertical motion of 10 mm of the platform was set to various frequencies between 1-5 Hz, simulating sudden motion of a patient. The vertical motion was repeated up and down 10 times for each frequency investigated. Additionally, the surface imaging system was used for motion monitoring during FLASH-RT for 11 canine patients of various breeds with shallow

situated tumors treated at the Elekta Precise linac. The canine patients were anesthetized prior to treatment and prescribed doses of 28-35 Gy. The total treatment times were ≤ 0.3 s. The treatment of the canine patients was approved by the Local Ethical and Administrative Committee at Department of Veterinary Clinical Sciences, University of Copenhagen, the Danish Experimental Animals Inspectorate (2020-15-0201-00429), the Animal Experiments Committee in Lund, Malmö (5.8.18-14316/2021), and the Swedish Board of Agriculture (reference number 5.2.18-02830/2020). An informed written consent form was also signed by all owners. The surface imaging system camera parameters for integration time and gain were individually optimized to enable as large detectable surface as possible for various fur colors and structures. The motion of the surface, well representing the shallow treatment volume, was monitored during the time from the confirmed setup at the treatment couch until after the treatment fraction was delivered. All motion data was analyzed by retrieving data from the Catalyst™ system log files.

Initial data showed that the simulated phantom breathing motion could be measured and verified by the surface imaging Catalyst™ system within 0.6 mm using all the fur-like materials at SSD 70 and 100 cm, respectively. The result from the detection of a simulated sudden motion of a patient at SSD 70 cm is presented for the various fur-like blankets in Figure 4. For the lowest frequency investigated, the surface imaging system detected the motion pattern very well regardless of fur-like material. However, with increased frequency, the surface imaging system ability to detect the motion pattern deteriorated. Nevertheless, the system managed to detect a motion, which might be enough for the system to indicate a “beam-hold” of the FLASH-RT delivery. For 10 out of the 11 canine patients receiving surface guided FLASH-RT, the total vector deviation in lateral, longitudinal and vertical directions ($\sqrt{\Delta lat^2 + \Delta long^2 + \Delta vert^2}$) was within 2 mm from planned setup position, measured from the point at which the setup position was approved in the treatment room until approximately 10 s after beam delivery (Figure 5). Patient 5 had the largest measured motion, but also the poorest surface coverage, thus the interpretation of the motion data was uncertain for this case. It was generally a challenge to obtain an adequate surface image for the canine patients due to different fur structures, lengths, and colors. For the patient cases with very dark fur a long integration time was necessary, which decreased the speed of the surface imaging system. Shorter integration time in those cases resulted in decreased reconstructed surface regions. For one of the patients motion up to 3 cm was recorded prior to beam on and the treatment was postponed until sufficient anesthesia had been administered. The FLASH-RT beam was delivered once the total vector deviation had been below the tolerance level of 10 mm for approximately one minute (Figure 6). The total vector deviation reported by the surface imaging system was 0.10 mm 1.72 s before beam-on and 1.63 s afterwards.

We have shown preliminary data demonstrating that motion management during FLASH-RT is important and feasible using the SGRT system Catalyst™. The surface imaging system showed to be feasible for motion monitoring of canine patients with various types of fur in off-isocentric electron FLASH-RT treatments. Presented phantom-studies indicated that the system also could detect sudden vertical motion, which could potentially result in a beam-hold until the patient is in the planned position. Furthermore, our surface guided FLASH-RT study for 11 canine patients showed that the motion monitoring system could be used to estimate the motion prior to treatment and to assure that the patient remains in the correct position during beam delivery. It should be noted that only shallow targets were treated with the electron FLASH beam in this study. For deep seated targets the additional complexity of internal target and organs-at-risk motion need further considerations.

4. Overall summary & concluding remarks

The technical development within radiotherapy during the last decades has allowed us to treat cancer patients successfully with decreased acute and long-term radiation-induced side effects. For further improvement, we need to increase the therapeutic window even more. A novel proposal is to use ultra-high dose rate irradiation, i.e., FLASH, since several preclinical studies recently showed less normal tissue toxicity than conventional dose rate radiotherapy and with maintained tumour effect. However, since the magnitude of the so-called FLASH effect varies between studies there is a need for further

investigations. Also, standardised protocols for ultra-high dose rate (UHDR) beam dosimetry need to be established. Once the dosimetry can be completely controlled, the probability to fully understand the mechanism of the FLASH effect would increase, facilitating a clinical translation. The existing standard detector systems within the field of conventional radiotherapy meet severe challenges in FLASH-RT due to the ultra-high dose rate. Recently, published reviews and other novel studies present both suggested correction strategies and new promising detector candidates for UHDR beam dosimetry.

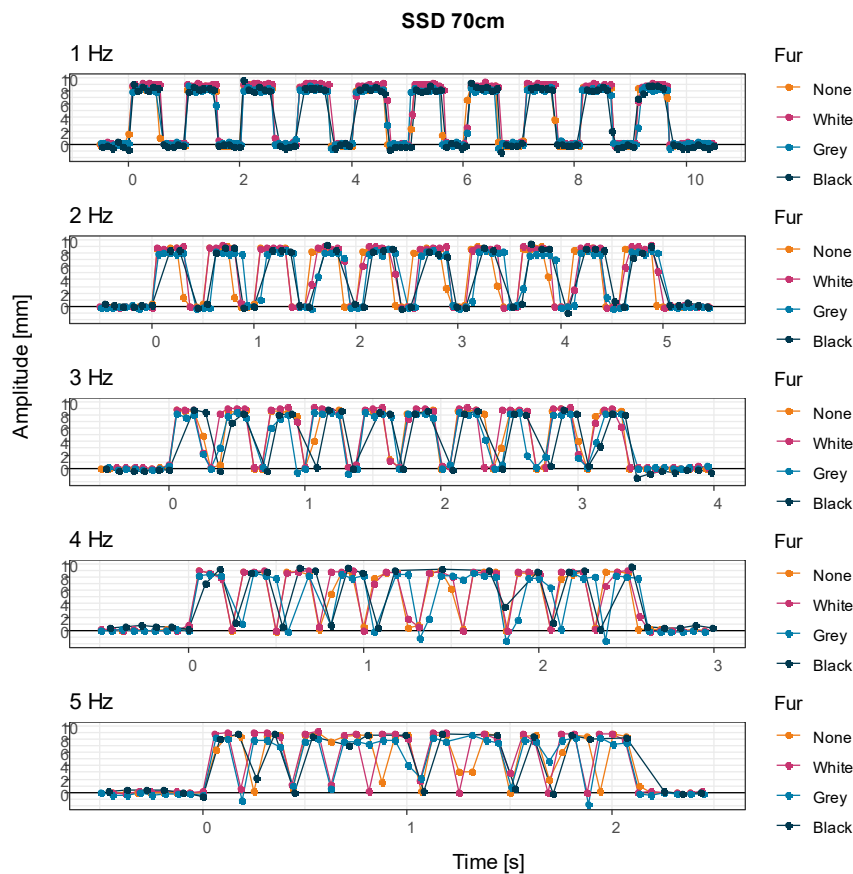


Figure 4. Surface imaging system Catalyst™ motion monitoring result presented as vertical motion as a function of time for various fur-like blankets on a platform that moves vertically at various frequencies (1-5 Hz). The measurements were carried out at our electron FLASH-RT setup, i.e., at SSD 70 cm.

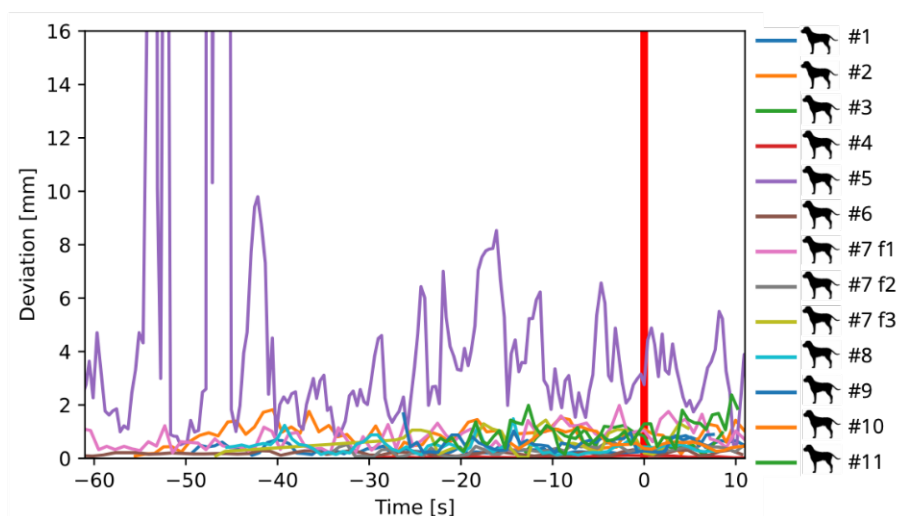


Figure 5. Motion data for 11 canine patients; the total vector of deviations in lateral, longitudinal and vertical directions as a function of time. The red line denotes beam-on normalized to time = 0 s to enable data visualization and comparison.

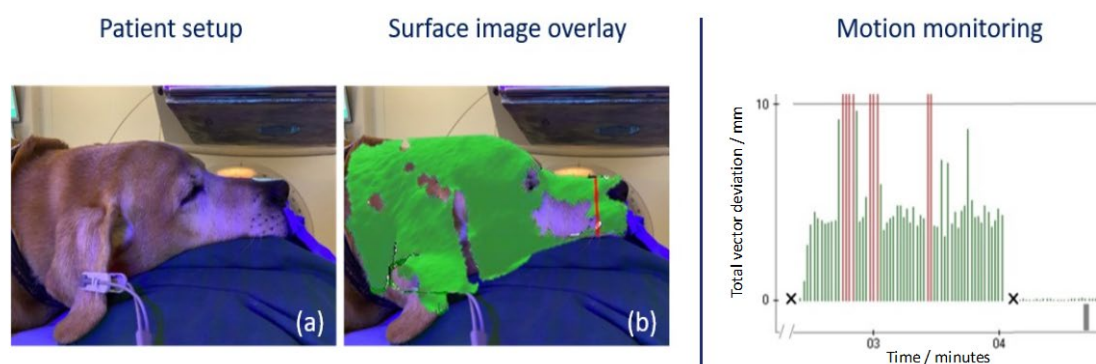


Figure 6. Left panel: The setup of a canine cancer patient (a), overlaid with the resulting surface image (b). Right panel: Real-time position (mm) relative to planned position over time (min); red bars indicate motion exceeding tolerance of 10 mm and the grey bar indicates the time for beam on [40].

It is not trivial to investigate the suitability of detector systems for UHDR beam dosimetry. Having the unique beam characteristics in mind, the dose rate dependence, as well as the spatial- and time-resolution are three important parameters of the system that need to be highlighted. All the luminescence-based dosimeters, such as the TLD, OSLD and Cherenkov-based detectors, as well as some of the chemical-based ones, such as radiochromic film and alanine, show outstanding dose rate independence. Although some of these (all but Cherenkov dosimetry) have rather long read-out times, they may still be suitable for passive FLASH measurements. Radiochromic film provides the best spatial resolution and is also tissue equivalent. Cherenkov dosimetry, with a ps time resolution and high 2D spatial resolution, was recently discussed as an ideal candidate for online FLASH-RT dosimetry. Charge-based detectors, such as diodes and diamonds, also have high time resolution, which makes them suitable for real-time dosimetry, although they are limited to point-dose measurements. Other unfavourable characteristics for charge-based detectors are their dose rate- and energy dependence and non-tissue equivalence. However, novel studies show that tuning of the physical properties of the diamonds can result in response linearity for UHDR irradiation. To conclude, the search for the ideal

detector system for dosimetry in FLASH beams is still ongoing to meet the need for standardised protocols for UHDR beam dosimetry.

In the meantime, we have started initial FLASH measurements using the 3D polymer gel dosimeter NIPAM. We plan to use electron-range modulating bolus in FLASH-RT, requiring a detector system with high spatial resolution for 3D dose verification. Our first feasibility tests showed the expected dose rate dependence. However, the response can be fitted by a quadratic polynomial (linear in the typical FLASH fraction dose range up to 25 Gy) and together with a suitable calibration method, the NIPAM gel dosimeter might work for FLASH dose verification in 3D. This study is ongoing. Regardless of the dosimetry system, once standardized procedures are established, the next challenge is to validate that the high fraction dose is delivered to the intended volume, given that the duration of the treatment is just a fraction of a second. We have utilized real-time motion monitoring using the in-room clinical optical surface imaging system Catalyst™ at our FLASH-modified Elekta linear accelerator. Our preliminary data showed that surface guided FLASH radiotherapy was feasible for canine patients with various types of fur in an off-isocentric FLASH radiotherapy setup. The surface imaging system ability to control the FLASH beam-hold is subject of an ongoing study.

Once an accurate dosimetry system for ultra-high dose rate beams is recognized, standardized dosimetry protocols are established, and a reliable motion management system for fast real-time monitoring is accessible, this would facilitate the clinical translation of accurate and safe FLASH radiotherapy.

5. References

- [1] van de Lindt TN *et al* 2022 *Radiother. Oncol.* **167** 285-291
- [2] Whitaker J *et al* 2022 *Trends Cardiovasc. Med.* **32** 287-296
- [3] Favaudon V *et al* 2014 *Sci. Trans. Med.* **6** 245ra93
- [4] Schüller E *et al* 2022 *Med. Phys.* **49** 2082-95
- [5] Omyan G *et al* 2020 *J. Cancer Res. Ther.* **16** 1203-9
- [6] Wilson J *et al* 2020 *Front. Oncol.* **9** 1563
- [7] Vozenin MC *et al* 2019 *Clin. Oncol.* **31** 407-15
- [8] Montay-Gruel P *et al* 2017 *Radiother. Oncol.* **124** 365-9
- [9] Levy K *et al* 2020 *Sci. Rep.* **10** 1-35
- [10] Fouillade C *et al* 2020 *Clin. Cancer Res.* **26** 1497-506
- [11] Bourhis J *et al* 2019 *Radiother. Oncol.* **139** 11-7
- [12] Simmons DA *et al* 2019 *Radiother. Oncol.* **139** 4-10
- [13] Montay-Gruel P *et al* 2021 *Clin. Cancer Res.* **27** 775-84
- [14] Vozenin MC *et al* 2019 *Clin. Can. Res.* **25** 35-42
- [15] Konradsson E *et al* 2021 *Front. Oncol.* **11** 658004
- [16] Diffenderfer ES *et al* 2022 *Med. Phys.* **49** 2039-54
- [17] Schüller E *et al* 2022 *Med. Phys.* **49** 2082-95
- [18] Romano F *et al* 2022 *Med. Phys.* **49** 4912-32
- [19] Schüller A *et al* 2020 *Physica Medica* **80** 134-50
- [20] Ashraf MR *et al* 2020 *Front. Phys.* **8** 328
- [21] Konradsson E *et al* 2020 *Radiat. Res.* **194** 580-586
- [22] Petersson K *et al* 2017 *Med. Phys.* **44** 1157-67
- [23] Cavallone M *et al* 2022 *Med. Phys.* **49** 4731-42
- [24] Gómez F *et al* 2022 *Med. Phys.* **49** 4705-14
- [25] Kranzer R *et al* 2022 *Phys. Med. Biol.* **67** 1361-6560/ac73d1
- [26] Marinelli M *et al* 2022 *Med. Phys.* **49** 1902-10
- [27] Konradsson E *et al* 2022 *J. Phys.: Conf. Ser.* **2167** 012003
- [28] Jorge PG *et al* 2019 *Radiother. Oncol.* **139** 34-9
- [29] Hachadorian RL *et al* 2022 *Med. Phys.* **49** 4018-25
- [30] Rahman M *et al* 2021 *Phys. Med. Biol.* **66** 135009

- [31] El Naqa I *et al* 2022 *Med. Phys.* **49** 4109-22
- [32] Bourhis J *et al* 2019 *Radiother. Oncol.* **139** 18-22
- [33] Gondré M *et al* 2020 *Radiat. Res.* **194** 573-9
- [34] Jaccard M *et al* 2017 *Med. Phys.* **44** 725-35
- [35] Jirasek A *et al* 2015 *Phys. Med. Biol.* **60** 4399-411
- [36] Waldenberg C *et al* 2017 *J. Phys.: Conf. Ser.* **847** 012063
- [37] Li H *et al* 2022 *Med. Phys.* **49** e50-81
- [38] Bissonnette JP *et al* 2010 *Radiother. Oncol.* **96** 139-44
- [39] Batista V *et al* 2022 *Tech. Innov. Patient Support Radiat. Oncol.* **22** 1-8
- [40] Mannerberg A *et al* 2021 *Radiother. Oncol.* **161** (suppl 1) PO-1767
- [41] Batista V *et al* 2020 *Radiother. Oncol.* **153** 34-42
- [42] Al-Hallaq HA *et al* 2022 *Med. Phys.* **49** e82-112
- [43] Klein EE *et al* 2009 *Med. Phys.* **36** 4197-212
- [44] Karlsson A *et al* 2004 *J. Phys.: Conf. Ser.* **3** 284
- [45] Ceberg S *et al* 2010 *Phys. Med. Biol.* **55** 4885-98
- [46] Ceberg S *et al* 2010 *J. Phys.: Conf. Ser.* **250** 012051
- [47] Lempart M *et al* 2019 *Radiother. Oncol.* **139** 40-45
- [48] Hill B *et al* 2002 *Phys. Med. Biol.* **47** 4233-246
- [49] Mannerberg A *et al* 2021 *Tech. Innov. Pat. Supp. Radiat. Oncol.* **19** 41-5
- [50] Haraldsson A *et al* 2020 *J. Appl. Clin. Med. Phys.* **21** 139-48
- [51] Kügele M *et al* 2019 *J. Appl. Clin. Med. Phys.* **20** 61-8
- [52] Kügele M *et al* 2018 *J. Appl. Clin. Med. Phys.* **19** 25-38
- [53] Pallotta S *et al* 2020 *Med. Phys.* **47** 6310-18